Paper

Deep Learning-based SNR Estimation for Multistage Spectrum Sensing in Cognitive Radio Networks

Sanjeevkumar Jeevangi, Shivkumar Jawaligi, and Vilaskumar Patil

Department of Electronics and Communication Engineering, Faculty of Engineering and Technology (Co-Ed), Sharnbasva University, India

https://doi.org/10.26636/jtit.2022.164922

Abstract — Vacant frequency bands are used in cognitive radio (CR) by incorporating the spectrum sensing (SS) technique. Spectrum sharing plays a central role in ensuring the effectiveness of CR applications. Therefore, a new multi-stage detector for robust signal and spectrum sensing applications is introduced here. Initially, the sampled signal is subjected to SNR estimation by using a convolutional neural network (CNN). Next, the detection strategy is selected in accordance with the predicted SNR levels of the received signal. Energy detector (ED) and singular value-based detector (SVD) are the solutions utilized in the event of high SNR, whilst refined non-negative matrix factorization (MNMF) is employed in the case of low SNR. CNN weights are chosen via the Levy updated sea lion optimization (LU-SLNO) algorithm inspired by the traditional sea lion optimization (SLNO) approach. Finally, the outcomes of the selected detectors are added, offering a precise decision on spectrum tenancy and existence of the signal.

Keywords — cognitive radio, improved NMF, LU-SLNO system, optimized CNN, spectrum sensing

Tab. 1. List of acronyms.

Abbreviation	Description
ACD	Auto-correlation based detector
AWGN	Additive white Gaussian noise
AOA	Arithmetic optimization algorithm
BES	Bald eagle search
CDF	Cumulative distribution function
CFD	Cyclostationary feature-based detector
CR	Cognitive radio
CNN	Convolutional neural network
CRN	Cognitive radio networks
DWT	Discrete wavelet transform
ED	Energy detector
FAR	False alarm probability
IoT	Internet of Things
HGS	Hunger games search
LA	Lion algorithm
LU-SLNO	Levy updated SLNO
MME	Maximum-minimum eigen value detectors
MAF	Moving average filtering
MSWF	Multistage Wiener filter
MNMF	Modified non-negative matrix factorization
MSS	Multi-band spectrum-sensing
NBSS	Numerous narrow-band spectrum sensing
PRO	Poor rich optimization
PUs	Primary user
PSD	Power spectral density
ROC	Receiver operating curve
RF	Radio frequency
SUs	Secondary user
SS	Spectrum sensing
SVD	Singular value based detector
SNR	Signal to noise ratio
SLNO	Sea lion optimization
TSA	Taylor series approximation
WF	Wiener filter
WBSS	Wide-band spectrum sensing

1. Introduction

The scarcity of radio spectrum in bands below 6 GHz is turning into a severe issue in current wireless communication technologies. Legal restrictions and static allotment of channels are the major issues resulting in the lack of viable radio spectrum [1], [2]. According to [3]–[5], under-utilization of the available spectrum is the root cause of spectrum scarcity [3]–[5]. By enabling unlicensed (secondary) users to access legacy networks, the cognitive radio (CR) technology promises to solve this spectrum shortage problem in situations in which the spectrum is underutilized by its licensed (primary) users [6]–[8].

The most important task in the CR phase is spectrum sensing (SS), or the precise locating of spectral holes (white spaces).

NBSS techniques, such as cyclo-stationary feature identification, energy identification, and matched filtering [9]–[12] have been the focus of recent research. Unfortunately, NBSS algorithms concentrate on taking advantage of spectral opportunities over a narrow frequency range. Cognitive radio networks (CRNs) need to take advantage of spectral opportunities over a wide frequency range, from hundreds of MHz to tens of GHz, in order to achieve the expected high throughput [8], [13], [14].

Another technique, known as WBSS, has received a lot of interest recently as well, and much research is currently conducted in this specific area [15], [16]. In general, it involves determining the frequency location of each sub-band of the sensed RF spectrum, regardless of the form of PSD, starting with wavelet decomposition for detecting matching sub-bands accessible for the SU [8], [17]. This paper aims to contribute in the following aspects:

– It presents the MSS-CRN system paradigm, in which CNN is used to measure SNR;
– After estimating SNR values, the detection scheme is chosen based on SNR at the receiver;
– SNR is categorized based on two threshold values. For high SNR, ED and SVD techniques are used, whereas for low SNR, MNMF is used;
– CNN weights are chosen in an optimum manner by using the LU-SLNO algorithm.

Table 1 summarizes the acronyms and abbreviations used in this paper.

2. Related Works

A multi-stage robust detector suitable for CR was reported by Kaliappan *et al.* [18]. For bands with lower and higher SNR, the selected model used two parallel connected detectors. ED and SVD were used for high SNR bands, while CFD and ACD were used for low SNR bands. According to empirical results, the suggested method beats previous models in terms of complexity.

Moayad *et al.* in [19] defined the spectrum accessing process as a multi-stage rate optimization/channel assignment. A novel resource-based channel assignment technique was developed allowing for the appropriate utilization of the available temporal frequency units. Additionally, this approach relied upon packet segmentation capabilities to significantly increase network throughput.

Jay *et al.* [20] introduced a three-part approach for analyzing localization (ROC)-based sensing performance of MSS: the best spectrum-sensing strategies maximized the area under ROC curves and could be used as a performance scale for another MSS method and to assess the energy costs of MSS. Haobo *et al.* in [21] introduced MSWF to improve effectiveness of the detection process. Additionally, based on total energy obtained from all routes, the specific locations were obtained. As such an approach did not call for the evaluation of noise variances, the selected model was resistant to noise uncertainty. The selected system has increased detection capabilities, making it suitable for CR appliances. Kim *et al.* [22] created a unique spectrum sensing and CR-sharing technique for IoT devices. A unique theory known as reciprocal fairness was developed to ensure spectrum sensing and CR sharing. The accepted model relied also on the game theory and turned out to be more effective than other examined models.

Edge identification and noise removal operations were carried out concurrently using DWT-oriented models developed by Abhishek *et al.* [8]. A MAF strategy was presented at various levels of DWT-oriented models in order to provide higher detection performance in low SNR scenarios. Low-scale DWT values were also used to obtain enhanced performance and shorter computational time. Compared to similar models, the suggested multi-task approach was simpler and more effective.

Rajput *et al.* [23] evaluated an adaptive covariance cut-off approach, comparing it against current techniques, such as energy detection and MME. Such parameters as accuracy and complexity of sensing ROC curves were taken into account there. Additionally, for every detector, the effects of the signal bandwidth in relation to the observation bandwidth were investigated. Vijayakumar and Malarvizhi [24] researched an SDR implementation of CR using an energy detector and a Wiener filter (WF) to eliminate self-interference. WF predicted the self-interfering signal which was then removed from the received signal before being moved to the energy detector. The outcomes show improvements in the probability of detection and improved efficiency.

Eappen and Geoffrey [25] introduced a hybrid PSO-GSA model to detect spectrum holes with improved energy utilization. The inclusion of mutation and crossover components in PSO-GSA enabled the recommended method to recognize spectral gaps efficiently, while maintaining optimum transmission capacity, sensor bandwidth, and spectral power density. Saber *et al.* [26] suggested a streamlined implementation of spectrum detection based on real signals produced by an Arduino Uno board and a 433 MHz ISM wireless transmitter. The received signal was detected using artificial neural networks, support vector machines, decision trees, and k-nearest neighbors, using five support vectors: linear, quadratic, cubic, medium Gaussian, and coarse Gaussian. The results showed that the use of machine learning, in particularly of SVM and ANN techniques, ensures better spectrum sensing capabilities.

Table 2 provides a summary of MSS for CRN evaluations, obtained from the literature. SVD with a high SNR level and a short sensing time suffers from synchronization problems [18]. The MAC protocol used in [19] improves throughput and spectrum efficiency, but only allows a limited basic rate on each channel. The binary search approach employed in [20], offers great detection performance, while consuming less energy. However, the setting threshold level needs optimization. The MSWF model researched in [21] achieves minimal complexity and good detection performance. How-

ever, perfect energy detection was not possible. The concept of reciprocal fairness from [22], which improved flexibility and lowered the throughput loss ratio, lacks a researched behavior model. Additionally, DWT used in [8] offers high SNR and increased FAR levels. However, shadowing effects remain unimproved. CDF, known from [23], offers high detection probability and high SNR, but has to be optimized in terms of its noise performance. In [24], a WF-based model was presented which offers improved accuracy and minimized overhead. However, certain functions need to be executed for a higher number of cycles. The hybrid PSO-GSA model presented in [25] to identify spectrum holes with better energy efficiency has good convergence and does not adhere to local optima, but its computational complexity grows with the population size. In [26], a streamlined implementation of spectrum detection based on authentic signals is proposed. The results demonstrate that using machine learning, particularly SVM and ANN techniques, will result in better spectrum sensing efficiency. Nevertheless, targeting categories overlap each other.

A new multi-stage detector is proposed for reliable signal and spectrum detecting devices. When deployed in an MSS-CRN, the process is designed as follows (Fig. 1):

– first, the sampled signal is subjected to SNR estimation,
– SNR is estimated using CNN,
– after evaluating SNR, SNR estimate of the message data is used to determine the tracking system,
– two levels of SNR are determined, MNMF is utilized with low SNR settings, while ED and SVD are used in high SNR scenarios,
– the LU-SLNO technique is used to select CNN weights in the best possible manner.

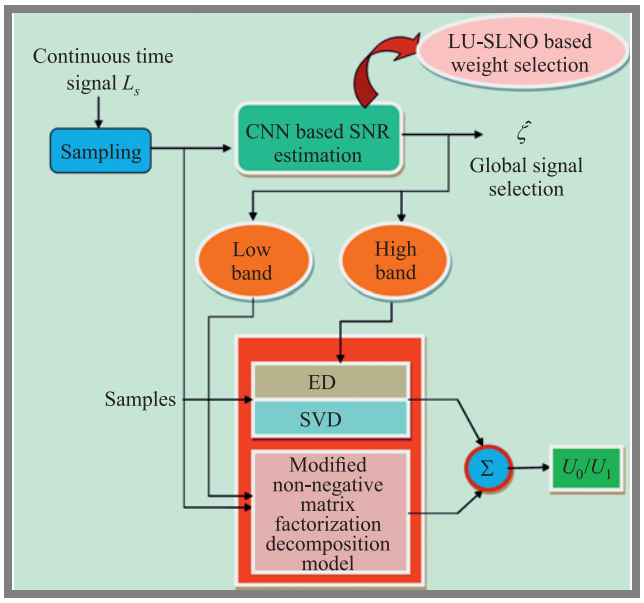

Fig. 1. MSS CRN system concept with LU-SLNO.

Tab. 2. Review of MSS in CRNs, based on existing papers.

Paper	Schemes developed	Features	Issues
[18]	SVD	• High SNR • Minimal sensing time	• Synchronization issues may occur
[19]	MAC protocol	• High spectrum efficiency • Enhanced throughput	• Each channel supports a predetermined basic rate only
[20]	Binary search method	• High detection performance • Minimized energy consumption	• Needs more consideration in terms of threshold selection
[21]	MSWF model	• Minimal complexity • High detection performance	• Ideal detection of energy could not be achieved
[22]	Reciprocal fairness concept	• Better flexibility • Minimized throughput loss ratio	• Need consideration in terms of behavior modeling
[8]	DWT	• Increased FAR • High SNR	• Shadowing effects are not considered
[23]	CDF	• High detection probability • Higher SNR	• Noise issues have to be improved
[24]	WF	• Avoids overhead • High accuracy	• Certain functionalities require running more cycles
[25]	PSO-GSA model	• Does not stick to local optima • Better convergence rate	• Increase in computational complexity when population size increases
[26]	ANN+SVM	• Better accuracy	• Overlap between target classes

3. CNN-based SNR Estimation

A common representation of the signal recognition formula may by determined as:

$$z(t) = \begin{cases} m(t), & U_0 \\ s(t) + m(t) & U_1 \end{cases}. \tag{1}$$

where, $z(t)$ refers to the received signal, signal to identify is noted by $s(t)$, $m(t)$ refers to AWGN, while U_0 and U_1 refer to null and positive hypotheses, respectively.

Based on the determined SNR of the incoming signal, the multi-stage detector chooses a suitable detection method. AWGN with zero mean δ and unity variance σ^2 degrades the arriving time domain signal. The estimating technique is based on the signal's sampled noise component variance extraction [27], [28].

SNR estimation is performed as follows:
– Calculate the square of count of samples

$$x(m) = (z(m))^2 \quad m = 1, 2. \ldots, L_s, \tag{2}$$

– Address $x(m)$ samples as a lower-order polynomial for TSA.
– Estimate noise difference σ_m^2 from the foremost coefficients of the appropriate polynomial.
– Calculate signal power $\hat{Q}_s$ as:

$$\hat{Q}_s = \frac{1}{L_s} \sum_{m=1}^{L_s} (z(m))^2 - \sigma_m^2. \tag{3}$$

– SNR ζ is approximated as:

$$\hat{\zeta} = 20 \log \left(\frac{\hat{Q}_s}{\sigma_m^2} \right). \tag{4}$$

3.1. CNN Based Training

The taxonomy of CNN accuracy is renowned to be excellent, particularly for visual sources. By convoluting the input image's features, a CNN can extract more relevant information and more detailed features, which should further increase the accuracy of SNR calculations. A CNN [29] comprises 3 layers: convolution, fully connected, and pooling layers with their features formulated as:

$$Z'_{r,t,w} = \mathrm{wet}_w^{l\ \mathrm{T}} PI_{r,t}^l = D_w^l, \tag{5}$$

where, wet_w^l is the weight, D_w^l is the bias of w-th the filter linked to the l-th layer. At the central location (r, t) of the l-th layer, patch input is indicated as $PI_{r,t}^l$. The activation value $\mathrm{act}_{r,t,w}^l$ related with convolutional features z_{rtw}^l and is calculated as:

$$\mathrm{act}_{r,t,w}^l = \mathrm{act}\left(Z_{r,t,w}^l\right). \tag{6}$$

In the pooling layer, function $\mathrm{pool}(\bullet)$ is linked with $\mathrm{act}_{m,h,w}^l$, and $c_{r,t,w}^l$ is calculated as:

$$C_{r,t,w}^l = \mathrm{pool}\left(\mathrm{act}_{m,h,w}^l\right), \quad \forall (m.h) \in \mathrm{NN}_{r,t} \tag{7}$$

in which $\mathrm{NN}_{r,t}$ is neighbor $s(r, t)$. The CNN loss CL is:

$$CL = \frac{1}{wn} \sum_{h=1}^{wm} l\left(\theta, C^{(h)}, F^{(h)}\right). \tag{8}$$

where the general constraint related with wet_w^l and D_w^l is denoted by θ. The output, the labels and the h-th input feature are denoted as $F^{(h)}$, $C^{(h)}$, and $PI^{(h)}$, respectively.

4. Proposed LU-SLNO Algorithm

The SLNO optimization method well-known from [30] illustrates sea lions' propensity to hunt. The algorithm is enhanced here to increase its effectiveness and convergence. Traditional optimization techniques have shown that self-improvement is beneficial [31]–[38]. Sea lions' delicate whiskers are a distinguishing feature that aids in pinpointing the precise location of their prey. Four stages of the process are defined: tracking, social hierarchy, attacking, and encircling prey to determine the properties of LU-SLNO.

The tracking method is defined as:

$$\mathrm{DIS} = \left| 2\vec{A}\vec{\Re}(t) - \vec{X}(t) \right|. \tag{9}$$

in which DIS denotes the distance between the sea lion and its prey, the vector position of the sea lion and the targeted prey is given by $\vec{X}(t)$ and $\vec{\Re}(t)$, while t denotes the present iteration. Conventionally, identifies an arbitrary vector. In LU-SLNO, is evaluated based on a sinusoidal chaotic map.

In each cycle, the sea lion pays more attention to the victim. Equation (10) specifies the numerical model of this process:

$$\vec{X}(t+1) = \vec{\Re}(t) = \mathrm{DIS}\,\aleph. \tag{10}$$

where $(t+1)$ denotes the future iteration and $\aleph$ is continuously minimized across the iterations from 0 to 2.

The vocalization phase is illustrated in Eqs. (11)–(13) which describe finding the food and inviting other sea lions to participate in a joint attack. The speed of the leader's sound is denoted as $\overrightarrow{X_{\text{leader}}}$ and the speed of sound in the air and in water is designated by $\vec{P}_2$ and $\vec{P}_1$, respectively.

$$\overrightarrow{X_{\text{leader}}} = \left| \frac{\vec{P}_1(1 + \vec{P}_2)}{\vec{P}_2} \right|, \tag{11}$$

$$\vec{P}_1 = \sin\theta, \tag{12}$$

$$\vec{P}_2 = \sin\phi. \tag{13}$$

In the exploration phase, the SLnO model performs a universal search when $\aleph > 1$, defined as:

$$\mathrm{DIS} = \left| 2\vec{B}\vec{X}_{\mathrm{rnd}}(t) - \vec{X}(t) \right|. \tag{14}$$

$$\vec{X}(t+1) = \overrightarrow{X_{\mathrm{rnd}}}(t) - \mathrm{DIS}\,\aleph. \tag{15}$$

If $(\overrightarrow{\mathrm{SP}_{\text{leader}}} > 0.25)$, the attacking phase is conducted.

The attacking phase is employed to describe how a sea lion assaults the prey:

$$\vec{X}(t+1) = \left| \vec{\Re}(t) - \vec{X}(t).\cos(2\pi l) \right| + \vec{\Re}(t), \tag{16}$$

where the distance between the sea lion and its prey is identified by $\vec{\Re}(t) - \vec{X}(t)$, the absolute value is denoted by $||$ and the random number is referred by l.

In LU-SLNO, the sea lion's attack is based on the Levy method and is given as:

$$\vec{X}(t+1) = \left| \vec{\Re}(t) - \vec{X}(t).\cos(2\pi l) \right| + \vec{\Re}(t) \oplus \mathrm{levy}(\alpha) \tag{17}$$

where $t_{\max}$ implies the maximal iteration, while ra_1 and ra_2 imply arbitrary integers. In addition, Cauchy's mutation is performed for better convergence.

$$\mathrm{levy}(\alpha) = 2\left(1 - \frac{t}{t_{\max}}\right) \frac{ra_1 \cdot \beta}{|ra_2|^{\frac{1}{2}}}. \tag{18}$$

5. Multi-stage Detector

For applications requiring reliable signal and spectrum detection, i.e. for tactical adaptive communication networks, a multi-stage integrated detector is proposed. In this method,

two detectors (SVD and ED) are connected in parallel for servicing higher SNR regions, while one detector (MNMF) is used for lower SNR regions. The high SNR band covers the $0\ldots-10$ dB range, while the low band deals with SNR of $-10\ldots-20$ dB.

For the higher SNR band, probability $\mathrm{pr}=1$ when the approximated SNR ζ exceeds -9 dB. Total probability of detection pd and average sensing time st are expressed by:

$$\mathrm{pd} = \max(p^{\mathrm{ed}}, p^{\mathrm{svd}}) \tag{19}$$

$$\mathrm{st} = (s^{\mathrm{ed}}, \mathrm{st}^{\mathrm{svd}}) \quad \text{for} \quad \mathrm{pd} \geqslant 0.9. \tag{20}$$

For the lower SNR band, i.e. when $(G_2 > \zeta > G_3$ if ζ is below 9 dB then $\mathrm{pr}=0$ and $(1-\mathrm{pr})=1$. Total probability of detection pd and average sensing time st are:

$$\mathrm{pd} = \max(p^{\mathrm{MNMF}}) \tag{21}$$

$$\mathrm{st} = (\mathrm{st}^{\mathrm{MNMF}}) \quad \text{for} \quad \mathrm{pd} \geqslant 0.9. \tag{22}$$

For energy detection estimation, signal samples are doubled and then concatenated to obtain the message signal. Next, using the determined detection threshold μ_1, noise energy is estimated as:

$$\mu_1 = \sqrt{2L_s}\sigma_m^2 P^{-1}(Q_{fa}) + L_s\sigma_m^2, \tag{23}$$

where $p^{-1}(\cdot)$ implies a converse P function and Q_{fa} implies FAR.

Finally, the decision is made on the basis of:

$$Z \rightarrow \begin{cases} \text{if} \quad \sum_{j=1}^{L_s} |z_i|^2 < \lambda_1, & U_0 \\ \text{else} & U_1 \end{cases}, \tag{24}$$

where z_j implies a j-th sample of $z(t)$.

5.1. SVD-Based Detection

The linear system signal processing approach and statistics greatly benefit from the SVD technique. It serves as an additional method for figuring out the matrix's eigenvalues [18], [39]–[42].

For SVD detection purposes, we start by choosing the columns count of matrix V, so that $k < V < L_s - k$, where k implies the number of dominating singular values [41]. In most cases, when there are several samples L_s, $V \leqslant 20$. In the second step, it is combined into a Hankel matrix HM, as:

$$HM = q(x+1-1) \;\; n = 1, 2, \ldots, L \;\text{ and }\; l = 1, 2, \ldots, N. \tag{25}$$

After factorizing the matrix, we obtain singular values, i.e. $\lambda_{\min}$ and $\lambda_{\max}$ and then calculate the threshold value λ_2 as:

$$\lambda_2 = \frac{\left(\sqrt{L_s}+\sqrt{V}\right)^2}{L_s}\left(1+\frac{O\left(\sqrt{L_s}+\sqrt{V}\right)^{-\frac{2}{3}}}{(L_s\cdot V)^{\frac{1}{6}}}\right). \tag{26}$$

where O implies the Tracy Widom's operation of Q_{fa} [41], [42]:

In the next step, the proportion with threshold λ_2 is evaluated. If $\lambda_{\max} = \lambda_{\min} > \lambda_2$, the signal is available and that proves the hypothesis. Otherwise, the signal is not present, pointing at U_0.

5.2. Modified NMF

NMF estimates the fundamental matrix $H(n \times l)$ and the coefficient matrix $W(k \times m)$ from the original matrix [43] $Y \approx HW$. A multi-variant linear equation serves as the foundation of NMF. Each column of Y is roughly portrayed as a linear fusion of the vector form of H:

$$Y_i = \sum_{j=1}^{k} H_j W_{ji}. \tag{27}$$

where, $i = 1, 2, \ldots$ column count in Y.

As per the modified NMF, W^* is computed by limiting the summary of values in each column of W to one, as:

$$w_{ij}^* = \frac{W_{ij}}{\sum_{l=1}^{k} W_{ij}} \;\text{ or }\; \frac{\sum_{l=1}^{m} Wt_i}{\sum_{i=1}^{k} \frac{wt_i}{W_{ij}}}, \tag{28}$$

where wt refers to weight.

5.3. Sensing Time

The effectiveness of the suggested detection method is evaluated using st and pd metrics. The proposed st detector is formulated as:

$$\mathrm{st} = \mathrm{pr}\left(\mathrm{st}^{\mathrm{ed}}, \mathrm{st}^{\mathrm{svd}}\right) + (1-\mathrm{pr})\cdot \mathrm{st}^{\mathrm{MNMF}}. \tag{29}$$

where $\mathrm{st}^{\mathrm{ed}}$, and $\mathrm{st}^{\mathrm{svd}}$ refer to the mean sensing time of ED, SVD, and MNMF detectors, respectively.

6. Simulation Results

In order to simulate the effectiveness of CNN + LU-SLNO, Matlab was used together with the DeepSig dataset and radio ML 2016.10A from [44]. The simulation parameters and specifications are presents in Tab. 3, while representations of the sample signal used are shown in Fig. 2.

Tab. 3. Simulation parameters.

Parameter	Specification
Input signals	QPSK, BPSK, QAM64, PAM4
Channel	AWGN
SNR range	0 to -20 [dB]
High SNR region	0 [dB] >= x >= -9 [dB]
Low SNR region	-9 [dB] > x >= -20 [dB]
Detector used	ED, SVD (low SNR band) NMF (high SNR band)
Probability of false alarm P_{fa}	0.1

The proposed CNN + LU-SLNO model was validated over ANN+SVM [26], CNN+PSO-GSA [25], CNN + HGS, CNN + AOA, CNN + PRO, CNN + BES, CNN + LA, CNN + SLNO, AWGN (CFD) [18] and AWGN (ACD) [18], using a synthetic dataset created with GNU Radio and consisting of 11 modulations at different signal-to-noise ratios (8 digital and 3 analogue).

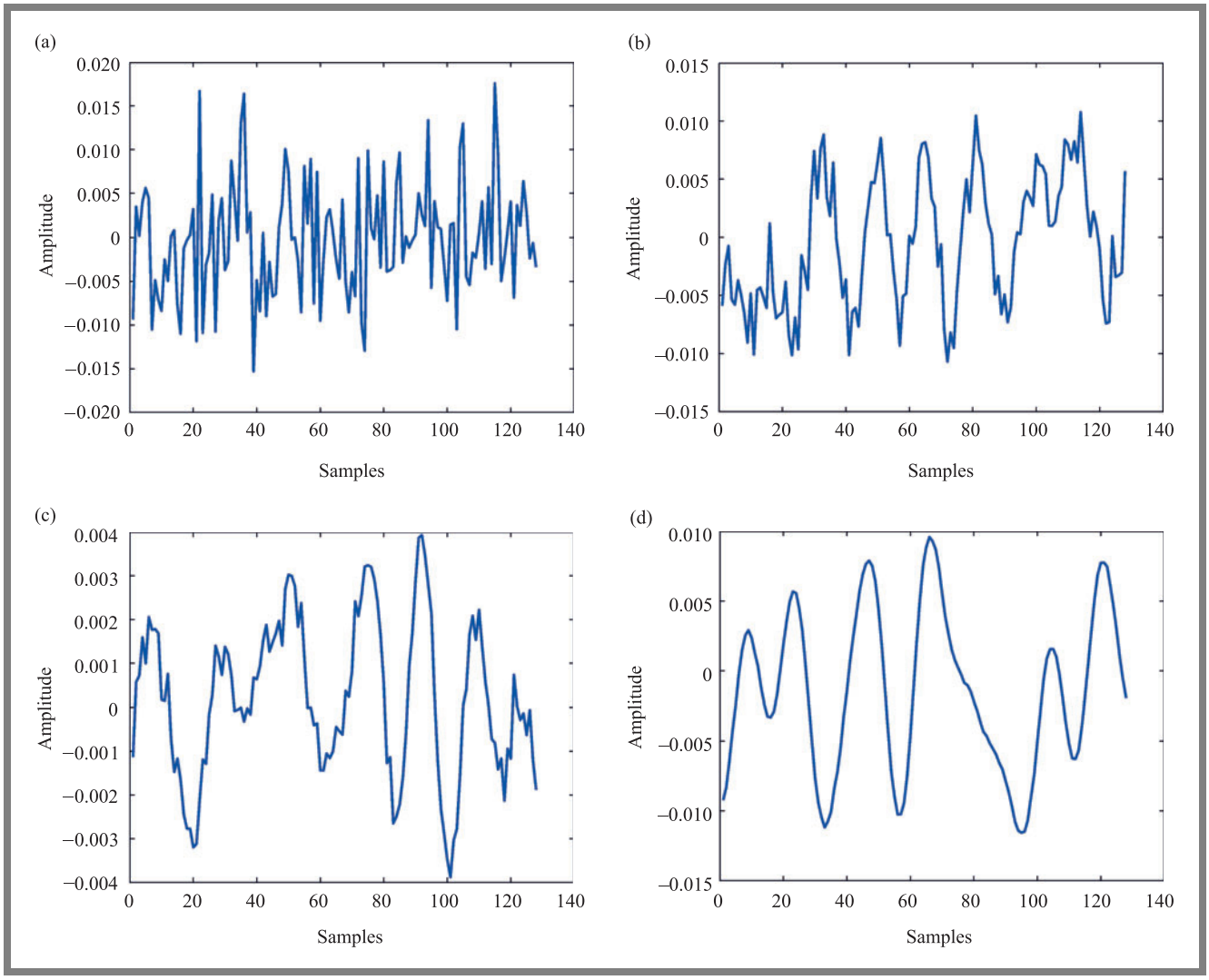

Fig. 2. Sample signal: a) BPSK, b) QPSK, c) PAM 4, and d) QAM 64.

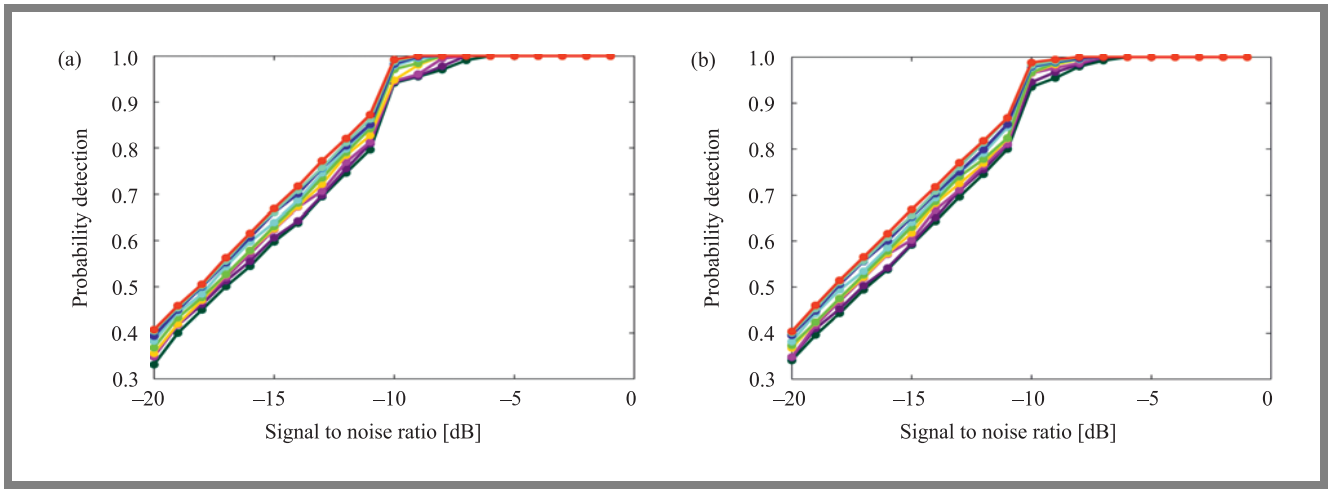

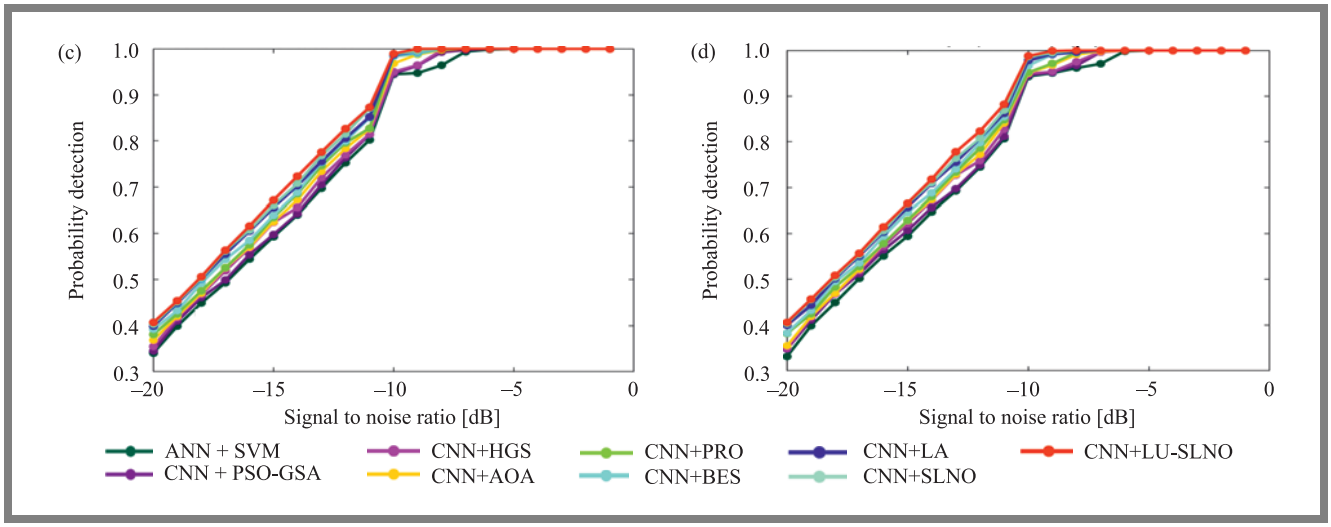

Fig. 3. Analysis of probability detection via CNN + LU-SLNO, compared with other schemes, for ED and: a) BPSK, b) PAM 4, c) QAM 64, d) QPSK.

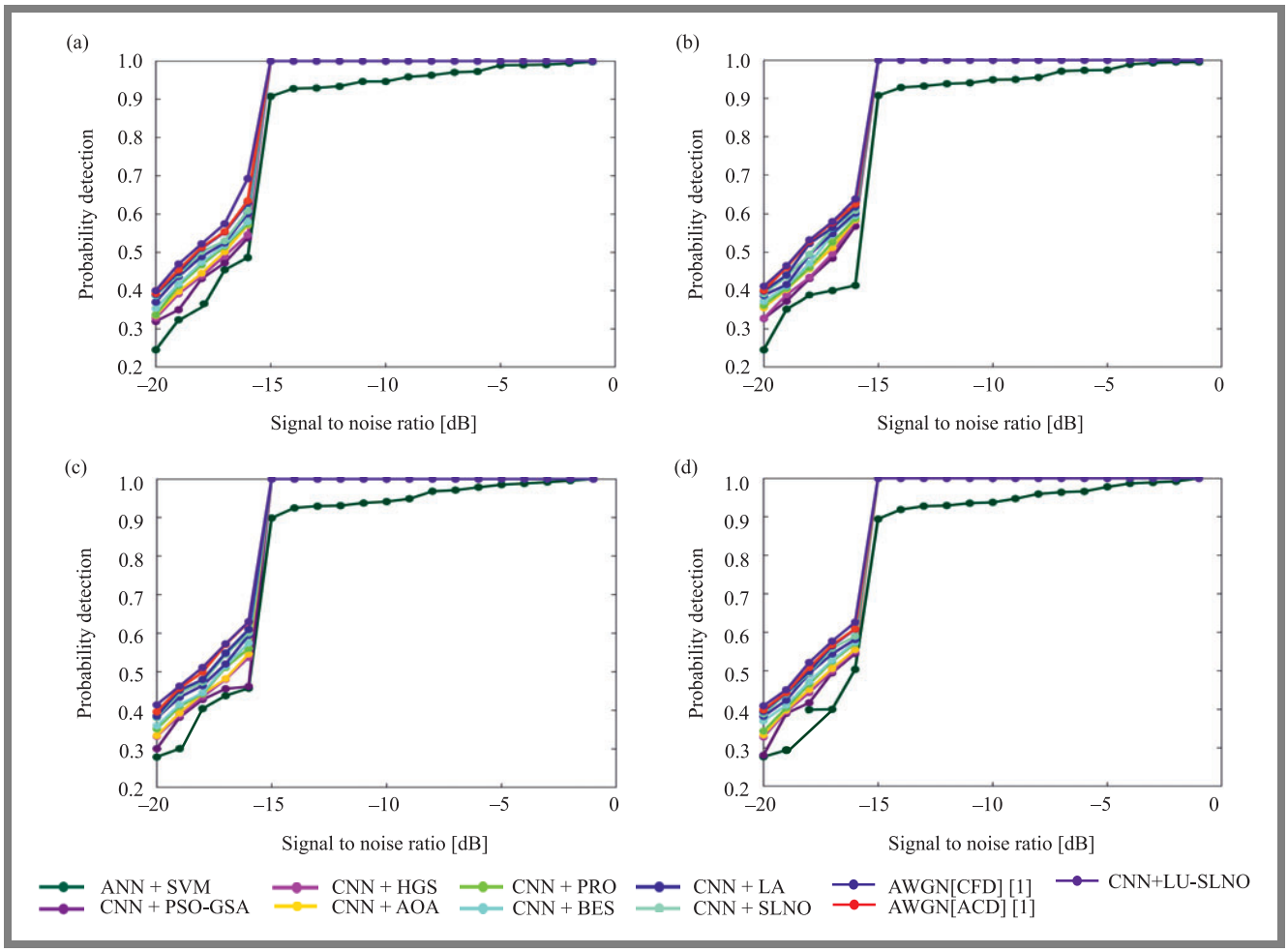

Fig. 4. Analysis of probability detection via CNN + LU-SLNO, compared with other schemes for MNHF and: a) BPSK, b) PAM 4, c) QAM 64, (d) QPSK.

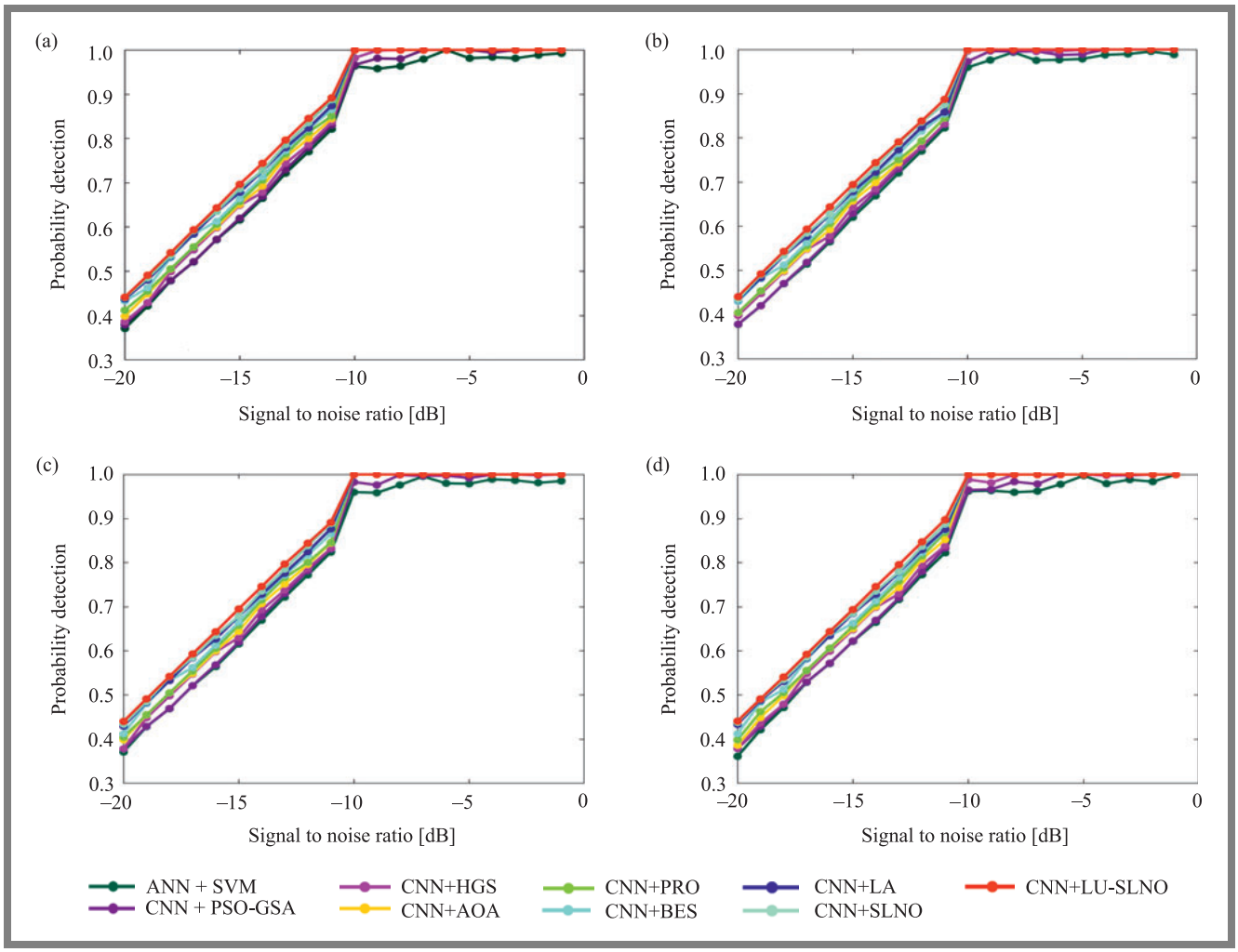

Fig. 5. Probability detection curves for CNN + LU-SLNO and SVD using: a) BPSK, (b) PAM 4, c) QAM 64, d) QPSK.

6.1. Analysis on Probability Detection

Probability detection is calculated in CNN + LU-SLNO using traditional systems with BPSK, QPSK, PAM 4, and QAM 64 modulation, as well as using conventional schemes pictured in Figs. 3–5.

Figure 3 analyzes the results obtained using ED. Fig. 4 presents the MNMF simulation, and Fig. 5 shows the analysis of SVD. Here, CNN + LU-SLNO shows outcomes that are superior to those achieved for other schemes. Better probability detection is clearly visible, and for all SNRs, probability detection using CNN + LU-SLNO equals nearly 1.

Tab. 4. Results of error rate statistical analysis.

Metrics	Std dev	Best	Variance	Mean	Worst
ANN+SVM	1.330	1.770	1.908	3.231	0.686
CNN+PSO-GSA	1.317	1.735	1.890	3.200	0.680
HGS	1.237	3.146	1.530	1.887	0.669
AOA	1.183	3.280	1.400	2.068	0.667
PRO	1.144	3.190	1.308	2.099	0.890
BES	1.004	3.155	1.008	2.125	1.103
LA	1.100	3.183	1.209	2.036	0.848
SLNO	1.196	3.137	1.431	1.936	0.818
LU-SLNO	1.263	3.110	1.595	1.815	0.666

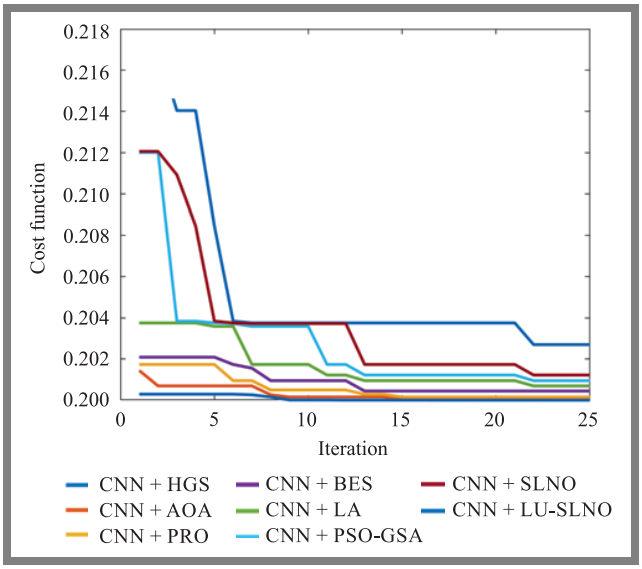

Fig. 6. Convergence analysis of LU-SLNO scheme and others method.

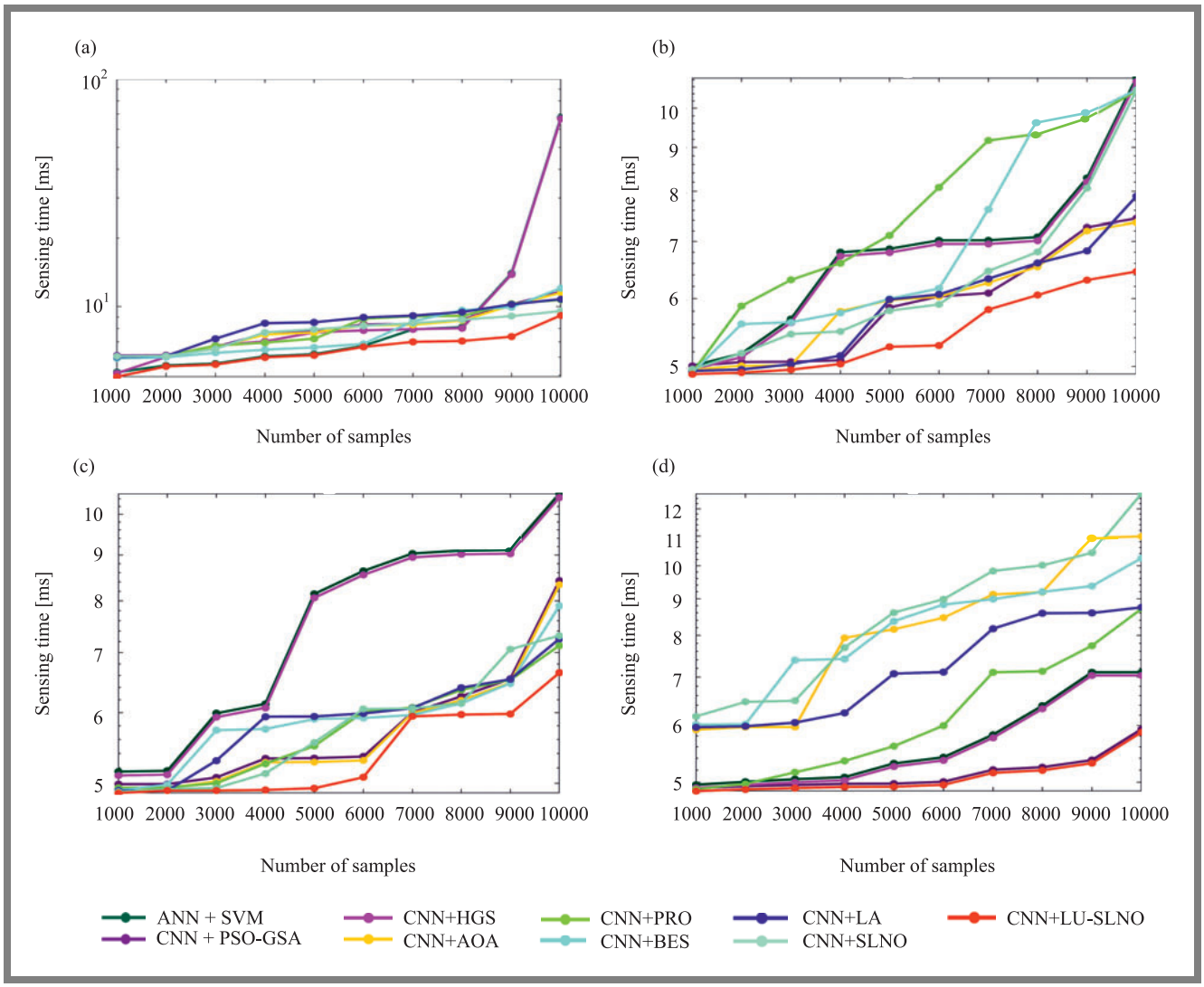

Fig. 7. Analysis of ED sensing time for CNN + LU-SLNO compared with other schemes for: a) BPSK, b) PAM 4, c) QAM 64, d) QPSK.

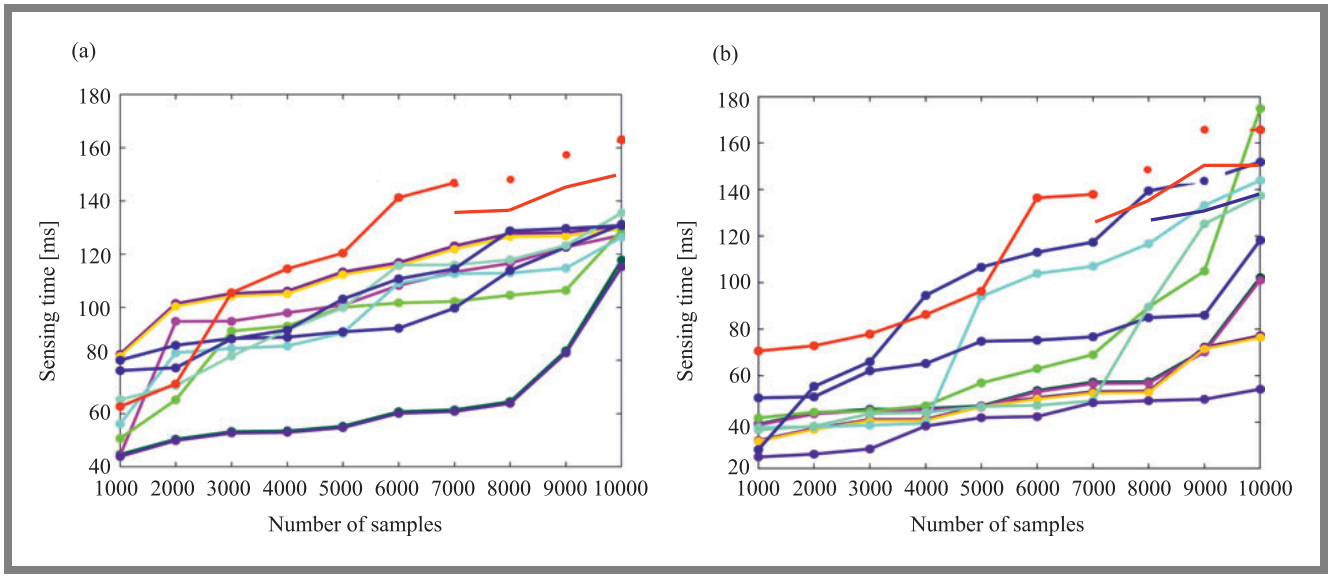

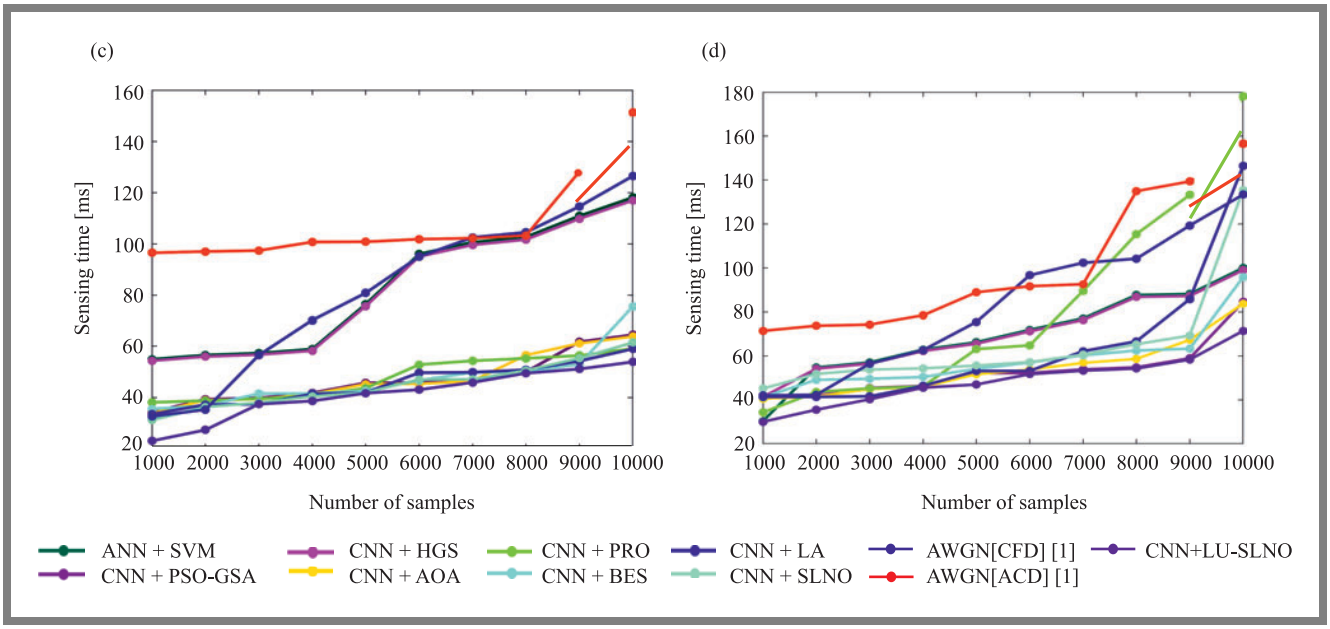

Fig. 8. Analysis of sensing time for CNN + LU-SLNO and other schemes (MNMF) for: a) BPSK, b) PAM 4, c) QAM 64, d) QPSK.

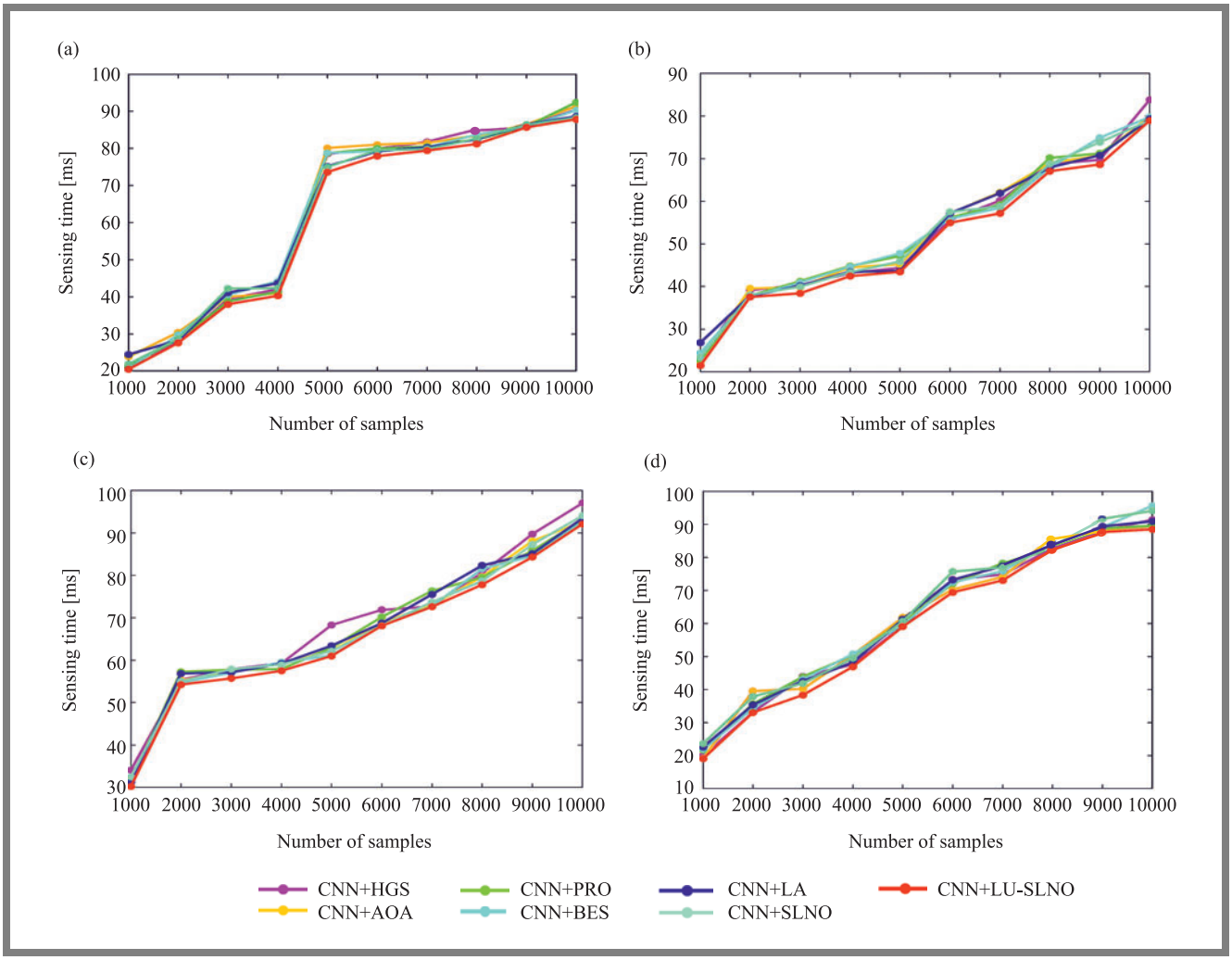

Fig. 9. Analysis of SVD sensing time for CNN + LU-SLNO compared with other schemes for: a) BPSK, b) PAM 4, c) QAM 64, d) QPSK.

6.2. Statistical Analysis

Table 4 summarizes the statistical analysis of CNN + LU-SLNO versus other schemes. CNN + LU-SLNO shows almost no gain in terms of its output error rate over its competitors.

6.3. Convergence Analysis

Figure 6 compares the cost of the LU-SLNO technique, for several iterations, with HGS, AOA, PRO, BES, LA, PSO-GSA, and SLNO. The cost of the LU-SLNO approach is lower for generations 0 to 25. In this case, the deployment of LU-SLNO results in lower convergence.

7. Sensing Time Analysis

The analysis of sensing time performed using the CNN + LU-SLNO method is presented in Figs. 7–9. The sensing time should be shorter to ensure improved system performance. The sensing time increases with the growing sample count. However, the sensing time using CNN + LU-SLNO is shorter when compared with others methods.

8. Conclusion

This article proposes a new MSS-CRN framework in which SNR estimation was relied upon in the channel selection process in cognitive radio. The detection strategy was selected in accordance with the estimated SNR of the received signal, using low and high values. For high SNR scenarios, ED and SVD were used, whereas for low SNR scenarios, MNMF was used. Together with the selected CNN weights and detectors, all SNRs and probability detection relying on CNN + LU-SLNO was superior than in other methods.

References

[1] S. Thompson, A-T. Fadi, K.J. Suresh, N. Balamurugan, and S. Sweta, "Artificial intelligence inspired energy and spectrum aware cluster based routing protocol for cognitive radio sensor networks", *Journal of Parallel and Distributed Computing*, vol. 142, pp. 90–105, 2020 (DOI: 10.1016/j.jpdc.2020.04.007).

[2] L.A. Vasquez-Toledo, B. Borja-Benítez, J. Alfredo, and Tirado-Mendez, "Mathematical analysis of highly scalable cognitive radio systems using hybrid game and queuing theory", *AEU – International Journal of Electronics and Communications*, vol. 127, Article 153406, 2020 (DOI: 10.1016/j.aeue.2020.153406).

[3] E.G. Carla, R.C. Mario, and K. Insoo, "Relay selection and power allocation for secrecy sum rate maximization in underlying cognitive radio with cooperative relaying NOMA", *Neurocomputing*, 2021 (DOI: 10.1016/j.neucom.2020.08.082).

[4] G. Kamlesh, S.N. Merchant, and U.B. Desai, "A novel multistage decision fusion for cognitive sensor networks using AND and OR rules", *Digital Signal Processing*, vol. 42, pp. 27–34, 2015 (DOI: 10.1016/j.dsp.2015.04.).

[5] J. Qadir, A. Baig, A. Ali, and Q. Shafi, "Multicasting in cognitive radio networks: Algorithms, techniques and protocols", *Journal of Network and Computer Applications*, vol. 45, pp. 44–61, 2014 (DOI: 10.1016/j.jnca.2014.07.024).

[6] S.M. Budaraju and M.A. Bhagyaveni, "A novel energy detection scheme based on channel state estimation for cooperative spectrum sensing", *Computers and Electrical Engineering*, vol. 57, pp. 176–185, 2017 (DOI: 10.1016/j.compeleceng.2016.08.017).

[7] R. Sekaran, S.N. Goddumarri, and D. Gupta, "5G Integrated Spectrum Selection and Spectrum Access using AI-based Frame work for IoT based Sensor Networks", *Computer Networks*, vol. 186, 2020 (DOI: 10.1016/j.comnet.2020.107649).

[8] A. Kumar, S. Saha, and R. Bhattacharya, "Wavelet transform based novel edge detection algorithms for wideband spectrum sensing in CRNs", *AEU – International Journal of Electronics and Communications*, vol. 84, pp. 100–110, 2017 (DOI: 10.1016/j.aeue.2017.11.024).

[9] S.N. Kumar and K. Bikshalu, "An extensive survey on cognitive radio based spectrum sensing using different algorithms", *Materials Today: Proceedings*, 2020 (DOI: 10.1016/j.matpr.2020.11.482).

[10] P. Feng, Y. Bai, and C. Liu, "A rapid coarse-grained blind wideband spectrum sensing method for cognitive radio networks", *Computer Communications*, vol. 166, pp. 234–243, 2020 (DOI: 10.1016/j.comcom.2020.11.015).

[11] R. Ahmed, Y. Chen, and L. Du, "CR-IoTNet: Machine learning based joint spectrum sensing and allocation for cognitive radio enabled IoT cellular networks", *Ad Hoc Networks*, vol. 112, Article 102390, 2020 (DOI: 10.1016/j.adhoc.2020.102390).

[12] G.P. Aswathy, K. Gopakumar, and T.P. Imthias Ahamed, "Joint sub-Nyquist wideband spectrum sensing and reliable data transmission for cognitive radio networks over white space", *Digital Signal Processing*, vol. 101, Article 102713, 2020 (DOI: 10.1016/j.dsp.2020.102713).

[13] E. Geoffrey and T. Shankar, "Hybrid PSO-GSA for energy efficient spectrum sensing in cognitive radio network", *Physical Communication*, vol. 40, Article 101091, 2020 (DOI: 10.1016/j.phycom.2020.101091).

[14] M.A. Osameh, M.A. Hisham, and A-M. Haithem, "Efficient on-demand spectrum sensing in sensor-aided cognitive radio networks", *Computer Communications*, vol. 156, pp. 11–24, 2020 (DOI: 10.1016/j.comcom.2020.03.032).

[15] K. Alok, T. Prabhat, and G. Singh, "Threshold selection and cooperation in fading environment of cognitive radio network: Consequences on spectrum sensing and throughput", *AEU – International Journal of Electronics and Communications*, vol. 117, Article 153101, 2020 (DOI: 10.1016/j.aeue.2020.153101).

[16] Y. Gao, C. Wang, and X. Bai, "GLRT-based spectrum sensing by exploiting multitaper spectral estimation for cognitive radio network", *Ad Hoc Networks*, vol. 109, Article 102289, 2020 (DOI: 10.1016/j.adhoc.2020.102289).

[17] K.G. Walid and S. Suzan, "Performance evaluation of cooperative eigenvalue spectrum sensing GLRT under different impulsive noise environments in cognitive radio", *Computer Communications*, vol. 160, pp. 567–576, 2020 (DOI: 10.1016/j.comcom.2020.06.033).

[18] K. Mourougayane, B. Amgothu, and S. Srikanth, "A robust multistage spectrum sensing model for cognitive radio applications", *AEU – International Journal of Electronics and Communications*, vol. 110, Article 152876, 2019 (DOI: 10.1016/j.aeue.2019.152876).

[19] M. Aloqaily, H. Bany, S. Jalel, and B. Othman, "A multi-stage resource-constrained spectrum access mechanism for cognitive radio IoT networks: Time-spectrum block utilization", *Future Generation Computer Systems*, vol. 110, pp. 254–266, 2020 (DOI: 10.1016/j.future.2020.04.022).

[20] J.B. Patel, S. Collins, and B. Sirkeci-Mergen, "A framework to analyze decision strategies for multi-band spectrum sensing in cognitive radios", *Physical Communication*, vol. 42, Article 101139, 2020 (DOI: 10.1016/j.phycom.2020.101139).

[21] H. Qing, H. Li, and Y. Liu, "Multistage Wiener filter aided MDL approach for wideband spectrum sensing in cognitive radio networks", *AEU – International Journal of Electronics and Communications*, vol. 73, pp. 165–172, 2017 (DOI: 10.1016/j.aeue.2017.01.012).

[22] S. Kim, "Inspection game based cooperative spectrum sensing and sharing scheme for cognitive radio IoT system", *Computer Communications*, vol. 105, pp. 116–123, 2017 (DOI: 10.1016/j.comcom.2017.01.015).

[23] R.S. Rajput, R. Gupta, and A. Trivedi, "An Adaptive Covariance Matrix Based on Combined Fully Blind Self Adapted Method for Cognitive Radio Spectrum Sensing", *Wireless Pers Commun*. vol. 114, pp. 93–111, 2020 (DOI: 10.1007/s11277-020-07352-9).

[24] P. Vijayakumar, S.W. Malarvizhi, "Wide band Full Duplex Spectrum Sensing with Self-Interference Cancellation-An Efficient SDR Implementation", *Mobile Netw Appl 22*, pp. 702–711, 2017 (DOI: 10.1007/s11036-017-0844-7).

[25] E. Geoffrey and T. Shankar. "Hybrid PSO-GSA for energy efficient spectrum sensing in cognitive radio network", *Physical Communication*, vol. 40 101091, 2020 (DOI: 10.1016/j.phycom.2020.101091).

[26] M. Saber, A. El Rharras, R. Saadane, A. Chehri, N. Hakem, and H.A. Kharraz, "Spectrum sensing for smart embedded devices in cognitive networks using machine learning algorithms", *Procedia Computer Science*, vol. 176, pp. 2404–2413, 2020 (DOI: 10.1016/j.procs.2020.09.311).

[27] M. Taleb, A. Amei, M. Jian, and J. Yingtao, "On a new approach to SNR estimation of BPSK signals", *Int J Electron Telecommun*, vol. 58, no. 3, 273–278, 2012 (DOI: 10.2478/v10177-012-0038-).

[28] A. Ijaz, A.B. Awoseyila, and B.G. Evans, "Improved SNR estimation for BPSK and QPSK signals", *IEEE Electron Lett*, vol. 45, 16 (DOI: 10.1049/el.2009.1759).

[29] J. Gu, *et. al.*, "Recent advances in convolutional neural networks", *Pattern Recognition*, vol. 77, pp. 354–377, 2018 (DOI: 10.1016/j.patcog.2017.10.013).

[30] R.M.T. Masadeh, B.A. Mahafzah, and A.-A. Sharieh, "Sea Lion Optimization Algorithm", *International Journal of Advanced Computer Science and Applications*, vol. no. 10, pp. 388–395, 2019 (DOI: 10.14569/IJACSA.2019.0100548).

[31] B.R. Rajakumar, "Impact of Static and Adaptive Mutation Techniques on Genetic Algorithm", *International Journal of Hybrid Intelligent Systems*, vol. 10, no. 1, pp. 11–22, 2013 (DOI: 10.3233/HIS-120161).

[32] B.R. Rajakumar, "Static and Adaptive Mutation Techniques for Genetic algorithm: A Systematic Comparative Analysis", *International Journal of Computational Science and Engineering*, vol. 8, no. 2, pp. 180–193, 2013 (DOI: 10.1504/IJCSE.2013.053087).

[33] S.M. Swamy, B.R. Rajakumar, and I.R. Valarmathi, "Design of Hybrid Wind and Photovoltaic Power System using Opposition-based Genetic Algorithm with Cauchy Mutation", *IET Chennai Fourth International Conference on Sustainable Energy and Intelligent Systems (SEISCON 2013)*, 2013, (DOI: 10.1049/ic.2013.0361).

[34] G. Aloysius and B.R. Rajakumar, "APOGA: An Adaptive Population Pool Size based Genetic Algorithm", *AASRI Procedia – 2013 AASRI Conference on Intelligent Systems and Control (ISC 2013)*, vol. 4, pp. 288–296, 2013, (DOI: 10.1016/j.aasri.2013.10.043).

[35] B.R. Rajakumar and G. Aloysius, "A New Adaptive Mutation Technique for Genetic Algorithm", *In proceedings of IEEE International Conference on Computational Intelligence and Computing Research (ICCIC)*, pp. 1–7, 2012 (DOI: 10.1109/ICCIC.2012.6510293).

[36] B.W. Mukund and N. Gomathi, "Improved GWO-CS Algorithm-Based Optimal Routing Strategy in VANET", *Journal of Networking and Communication Systems*, vol. 2, no. 1, pp. 34–42, 2019 (DOI: 10.46253/jnacs.v2i1.a4).

[37] H.B. Sadashiv, S.F. Kodad, S.K. Ambekar, and D. Manjunath, "Enhanced Invasive Weed Optimization Algorithm with Chaos Theory for Weightage based Combined Economic Emission Dispatch", *Journal of Computational Mechanics, Power System and Control*, vol. 2, no. 3, pp. 19–27, 2019 (DOI: 10.46253/jcmps.v2i3.a3).

[38] N.J. Amolkumar and N. Gomathi, "DIGWO: Hybridization of Dragonfly Algorithm with Improved Grey Wolf Optimization Algorithm for Data Clustering", *Multimedia Research*, vol. 2, no. 3, pp. 1–11, 2019 (DOI: 10.46253/j.mr.v2i3.a1).

[39] M.H. Omar, H. Suhaidi, and A.N. Shahrudin, "Eigenvalue-based signal detectors performance comparison", *The 17th Asia Pacific conference on communications*, 2011 (DOI: 10.1109/APCC.2011.6477853).

[40] Z. Yonghong and C.L. Ying, "Eigenvalue-based spectrum sensing algorithms for cognitive radio", *IEEE Trans Commun 2009*, 57(6), pp. 1784–1793 (DOI: 10.1109/TCOMM.2009.06.070402).

[41] M.H. Omar, H. Suhaidi, A. Angela, and A.N. Shahrudin, "SVD based signal detector for cognitive radio networks", *13th International conference on computer modeling and simulation*, 2011 (DOI: 10.1109/UKSIM.2011.104).

[42] Z. Yonghong and C.L. Ying, "Maximum-minimum eigenvalue detection for cognitive radio", *IEEE eighteenth international symposium on personal, indoor and mobile radio communications*, pp. 1–5 2007 (DOI: 10.1109/PIMRC.2007.4394211)

[43] Y. Liu, Y. Liang, Q. Kuang, F. Xie, Y. Hao, Z. Wen, and M. Li, "Post-modified non-negative matrix factorization for deconvoluting the gene expression profiles of specific cell types from heterogeneous clinical samples based on RNA-sequencing data", *Journal of Chemometrics*, e2929, 2017 (DOI: 10.1002/cem.2929).

[44] –, https://www.kaggle.com/datasets/nolasthitnotomorrow/radioml2016-deepsigcom?resource=download.

Sanjeevkumar Jeevangi, Research Scholar

E-mail: sjeevangi8@gmail.com

Department of Electronics and Communication Engineering, Faculty of Engineering and Technology (Co-Ed), Sharnbasva University, India

Shivkumar Jawaligi, Professor and Dean

Department of Electronics and Communication Engineering, Faculty of Engineering and Technology (Co-Ed), Sharnbasva University, India

Vilaskumar Patil, Associate Professor

Department of Electronics and Communication Engineering, Faculty of Engineering and Technology (Co-Ed), Sharnbasva University, India